International Journal of Immunopathology & Pharmacology

Original Research Article

International Journal of Immunopathology and Pharmacology
Volume 32: 1–19

DOI: 10.1177/2058738418818630
journals.sagepub.com/home/iji
SAGE

Protective effects of *Panax notoginseng* saponins in a rat model of severe acute pancreatitis occur through regulation of inflammatory pathway signaling by upregulation of miR-181b

Ming-wei Liu[1], Yun-qiao Huang[1], Ya-ping Qu[2], Dong-mei Wang[3], Deng-yun Tang[3,4], Tian-wen Fang[2], Mei-xian Su[4,5] and Yan-qiong Wang[6]

Abstract

Panax notoginseng saponins are extracted from Chinese ginseng—*Panax notoginseng Ledeb*—and are known to have therapeutic anti-inflammatory effects. However, the precise mechanism behind their anti-inflammatory effects remains relatively unknown. To better understand how *Panax notoginseng* saponins exert their therapeutic benefit, we tested them in a rat model of severe acute pancreatitis (SAP). Rats received a tail vein injection of *Panax notoginseng* saponins and were administered 5% sodium taurocholate 2 h later. Pancreatic tissue was then harvested and levels of miR-181b, FSTL1, TREM1, TLR4, TRAF6, IRAK1, p-Akt, p-p38MAPK, NF-κBp65, and p-IκB-α were determined using Western blot and quantitative real-time polymerase chain reaction (qRT-PCR). Enzyme-linked immunosorbent assays were used to determine serum levels of tumor necrosis factor-α (TNF-α), TREM1, interleukin (IL)-6, ACAM-1, IL-8, and IL-12 and DNA-bound levels of NF-KB65 and TLR4 in pancreatic and ileum tissue. Serum levels of lipase and amylase, pancreatic myeloperoxidase (MPO) activity, and pancreatic water content were also measured. Hematoxylin and eosin staining was used for all histological analyses. Results indicated upregulation of miR-181b, but negligible levels of FSTL1, p-p38MAPK, TLR4, TRAF6, p-Akt, IRAK1, TREM1, p-NF-κBp65, and p-IκB-α, as well as negligible DNA-bound levels of NF-KB65 and TLR4. We also observed lower levels of IL-8, IL-6, ACAM-1, TNF-α, MPO, and IL-12 in the *Panax notoginseng* saponin–treated group when compared with controls. In addition, *Panax notoginseng* saponin–treated rats had significantly reduced serum levels of lipase and amylase. Histological analyses confirmed that *Panax notoginseng* saponin treatment significantly reduced taurocholate-induced pancreatic inflammation. Collectively, our results suggest that *Panax notoginseng* saponin treatment attenuated acute pancreatitis and pancreatic inflammation by increasing miR-181b signaling. These findings suggest that *Panax notoginseng* saponins have therapeutic potential in the treatment of taurocholate-induced SAP.

[1]Department of Emergency Medicine, The First Affiliated Hospital of Kunming Medical University, Kunming, China
[2]Postgraduate Department, Kunming Medical University, Kunming, China
[3]Yunnan Green Field Biopharmaceutical Co., Ltd., Kunming, China
[4]Skin Disease Prevention Institute of Wenshan Zhuang and Miao Autonomous Prefecture, Yunnan, China
[5]Emergency Intensive Care Unit, The Second Affiliated Hospital of Kunming Medical University, Kunming, China
[6]Department of Anesthesiology, The First Affiliated Hospital of Kunming Medical University, Kunming, China

Corresponding authors:
Ming-wei Liu, Department of Emergency Medicine, The First Affiliated Hospital of Kunming Medical University, No. 295, Xichang Road, Kunming 650032, Yunnan, China.
Email: lmw2004210@163.com

Mei-xian Su, Emergency Intensive Care Unit, The Second Affiliated Hospital of Kunming Medical University, 1 Mayuan Road, Kunming 650106, Yunnan, China.
Email: Kmsmx24@126.com

Keywords
acute pancreatitis, follistatin-like 1, miR-181b, *Panax notoginseng* saponins, taurocholate, triggering receptor expression on myeloid cells 1

Date received: 5 July 2018; accepted: 15 November 2018

Introduction

Severe acute pancreatitis (SAP) is a condition with many complications, resulting in a high death rate of between 20% and 30%.[1–5] However, acute pancreatitis (AP) is usually mild, has no complications, and usually heals on its own.[1] SAP has several significant pathological features, including a large area of necrotic tissue and extensive pancreatic hemorrhage.[2] Clinically, SAP is often accompanied by acute renal insufficiency, acute lung injury (ALI), and hepatic impairment.[3,4] Late-stage SAP features multiple organ dysfunction syndromes (MODS), and uncontrolled SAP can result in multiple organ failure (MOF).[3] Despite its significant health effects and high mortality rate, there remains no satisfactory treatment for SAP. Current therapeutic methods are purely symptomatic and focused on pain relief, gastric decompression, and the maintenance of balanced electrolytes, fluids, and pH.[6] Given this great therapeutic need, attention has recently turned to the active ingredients found in *Panax notoginseng*.[7] It has been hoped that of these, one might prove beneficial in the treatment of SAP.

Panax notoginseng is one of the most commonly used species in traditional Chinese medicines (TCMs) and has significant efficacy in treating pathological hemostasis, promoting blood circulation, and alleviating pain.[7,8] *Panax notoginseng* saponins are obtained from *Panax notoginseng* (Chinese ginseng) extracts and are primarily composed of ginsenosides (Rg1, Rb1, and Rg2), notoginsenoside R1, and RK3.[7] Ginsenoside Rb1 is an inhibitor of vascular cell adhesion molecule 1 (VCAM-1).[8] Several of these compounds have active biological properties; for instance, protopanaxadiol-type saponin is the most potent saponin fraction against tumor necrosis factor-α (TNF-α)-induced monocyte adhesion.[9] Moreover, ginsenoside Rb1 functions as a phytoestrogen and ginsenoside Rg1 has been shown to lower hepatic oxidative stress in exercising rats.[10,11] In addition, ginsenoside Rg1 protects against memory impairments.[12] *Panax notoginseng* is also an inhibitor of TNF-α-induced endothelial adhesion molecule expression and monocyte adhesion.[13] In apolipoprotein E (ApoE)-deficient mice, ginsenoside Rg2 also suppresses RAGE/MAPK signaling and helps block nuclear factor kappa B (NF-κB).[14] Finally, Rg1 and RK3 activate the phosphatidylinositol-3 kinase Akt pathway and inhibits p38 MAPK signaling.[8,15] Critically, *Panax notoginseng* saponins may be help slow or prevent inflammatory diseases; however, the mechanism(s) of action of *Panax notoginseng* with regard to disease modification remain relatively unknown.

MicroRNAs (miRNAs) are the primary regulators in a variety of biological processes.[16] Specific disease-related miRNAs that have been recently identified include those for several kinds of cancers, autoimmune diseases, and infectious diseases.[16–18] Additional related miRNA studies have verified some of these functions in vivo.[19–21] However, the role of miRNAs in inflammatory diseases like AP remains poorly understood. Relatedly, it is also necessary to better understand whether miR-181b functions as a cytokine-responsive miRNA in the regulation of the pancreatic response to inflammation.

Previous in vivo reports have shown that the FSTL1 protein significantly reduced pro-inflammatory mediator expression in the ischemic areas of the myocardium.[22] Additional in vitro work has extended these findings, showing that the treatment of either cultured cardiomyocytes or macrophages with FSTL1 protein decreased pro-inflammatory gene expression in response to lipopolysaccharide (LPS) application.[23]

The first identified member of the TREM family, TREM1, is widely expressed on pathogen-exposed myeloid cells.[24] Enhanced TREM1 expression promotes excessive inflammation and increases circulating chemokines and cytokines.

Here, we sought to evaluate the role of the miR-181b signaling pathway in taurocholate-induced AP. After taurocholate treatment, miR-181b signaling decreased, FSTL1 and TREM1 signaling pathways

were enhanced, and the levels of inflammatory gene and protein levels in the mouse pancreas were elevated. Collectively, these effects contributed to later pancreatic injury. Importantly, *Panax notoginseng* saponins enhanced miR-181b signaling, blocked FSTL1 and TREM1 activity, and reduced pancreatic injury. This led to a weaker presentation of AP. Taken together, our results demonstrate that *Panax notoginseng* saponins attenuated AP and pancreatic inflammation by increasing miR-181b signaling activity. Our study further suggests that the miR-181b signaling pathway functions as a protective factor in the development of AP.

Materials and methods

Reagents

A commercially available reverse transcription (RT) reaction kit (Takara Shuzo Co., Ltd., Kyoto, Japan) and a commercially available Trizol kit (Invitrogen, Carlsbad, CA, USA) were both used according to the manufacturer's instructions. Commercially available DNA markers and polymerase chain reaction (PCR) kit (Roche, South San Francisco, CA, USA) were also used according to the manufacturer's instructions. Rabbit polyclonal antibodies to FSTL1 and TREM1 were purchased from Sigma Chemical (St. Louis, MO, USA). Rabbit polyclonal anti-Akt, anti-p-Akt, and rabbit polyclonal anti-TLR4 antibodies were purchased from Cell Signaling Technology (Danvers, MA, USA), while rabbit polyclonal antibodies to TRAF6 and IRAK1 were purchased from American Diagnostica (Stamford, CT, USA). Rabbit polyclonal antibodies to p38MAPK and p-p38MAPK were purchased from Cell Signaling Technology). Rabbit polyclonal antibody to p-IRAK1 was purchased from Sigma Chemical, while rabbit polyclonal antibodies toNF-kBp65 and p-NF-kBp65 were obtained from Innovative Research (Southfield, MI, USA). Rabbit polyclonal antibodies to IκB-a and p-IκB-a were purchased from Abcam (Cambridge, MA, USA). Rabbit polyclonal β-actin was obtained from Promega (Madison, WI, USA). ACAM-1 and IL-12 enzyme-linked immune sorbent assay (ELISA) kits were obtained from BioLegend (San Diego, CA, USA), while TNF-α, interleukin (IL)-6, and IL-8 ELISA kits were obtained from the Science and Technology Development Center of the People's Liberation Army General Hospital (Beijing, China).

Drugs

Panax notoginseng saponin extracts were acquired from Yunnan Baiyao Group Co., Ltd. (Kunming, Yunnan, China, Approval No. Zhunzi Z5302149). All active compounds were identified and biochemical fingerprints obtained according to previously reported methods.[7–13] The main active components included notoginsenoside R1 and ginsenosides Rg1 and Rb1.

Cell culture

The pancreatic acinar cell line[25] was used to observe the in vitro effects of miR-181b on AP. Pancreatic acinar cells were freshly harvested from male Sprague Dawley rats (200–220 g) through enzymatic digestion using a previously described protocol.[26] The harvested pancreatic acinar cells were grown in DMEM containing 100 U/mL penicillin, 5% fetal bovine serum (FBS), 50 μg/L amphotericin B, and 100 U/mL streptomycin at 37°C in a humidified atmosphere containing 5% CO_2. Cells were cultured in six-well plates until they were subconfluent.

miRNA mimics, miRNA, inhibitors, and gene transfection

Pancreatic acinar cells were cultured to 40% confluence. miR-181b mimics, miR-181b mimic-negative control (NC), miR-181b inhibitor, and miR-181b inhibitor-NC (Invitrogen) were individually added to Lipofectamine 2000 (Invitrogen) and the resulting mixture was added to the cell medium. Total RNA and all proteins were obtained 24 h post-transfection and stored for later quantitative real-time polymerase chain reaction (qRT-PCR) and Western blot analyses.

miR-181b target gene prediction and dual luciferase reporter assay

Two software applications (PicTar, www.pictar.org and Target Scan, http://www.targetscan.org) and one database (www.mirbase.org) were used to determine possible miR-181b targets. Pancreatic acinar cells (1×10^5) were cultured in 24-well plates and transfected using Lipofectamine 2000 (Invitrogen) with one of the following: FSTL1, TREM1-3′UTR-wt, FSTL1, TREM1-3′ UTR-mt, mi-181b, or mi-NC. At 24 h post-transfection, a

luciferase activity was conducted using the Dual Luciferase Reporter Assay System (Promega). Results were then normalized to Renilla luciferase activity.

AdCMV-miR-181b administration

AdCMV-miR-181b was constructed as previously described.[27] A constitutively active miR-181b construct was administered (1×10^9 pfu of AdCMV-miR-181b) via tail intravenous injection into Sprague Dawley rats. Administration was followed by taurocholate-induced pancreatitis after 10 days post-intravenous (IV) administration of AdCMV-miR-181b. Control rats received an empty adenoviral vector and identical taurocholate exposure.

Animals

Adult male Sprague Dawley rats were obtained from Kunming Medical University Laboratory Animal Center (Kunming, China). All rats were housed in the Animal Care Facility of Kunming Medical University under pathogen-free conditions in controlled (30%–70%) humidity. Standard laboratory chow and water were provided ad libitum. In all experiments, 8- to 9-week-old rats were used. All experiments were approved by the Animal Care Committee of Kunming Medical University.

Taurocholate-induced SAP

Under aseptic conditions, rats were anesthetized using 1% pentobarbital sodium (i.p., 35 mg/kg body weight). SAP was modeled using a microinfusion pump containing 5% sodium taurocholate (1.5 mL/kg body weight). Taurocholate was administered at a rate of 0.2 mL/min according to previous reports.[28] Sham-operated animals underwent the same surgical procedures but did not have active infusion into the pancreas.

Animal groups and treatment

Rats (n = 32) were equally and randomly divided into the following four groups: sham-operated (SO), sham-operated with treatment (treatment SO), SAP model (model), and SAP model with treatment (treatment SAP). Treatment groups (treatment SO and treatment SAP) received a tail injection (50 mg/kg) of *Panax notoginseng* saponin extract every 8 h for 24 h. Normal control, sham, and control groups were given the same volume of saline according to the same injection schedule. After 24 h, all rats were anesthetized using 2.5% sodium pentobarbital (150 mg/kg; Wuhan Dinghui Chemical Co., Ltd., Wuhan, China) and the right internal carotid artery was isolated. Blood (5 mL) was extracted and then immediately centrifuged. The supernatant was collected, aliquoted into two sterile tubes, and stored at −20°C until later analysis. Ascites volume was acquired from the opened abdominal wall. Both serum and ascites fluid were used to establish amylase levels and ascitic capacity. After rapid cervical dislocation, ileum and pancreatic tissue were rapidly removed and fixed in 10% formalin for later histological analyses. Separate pancreatic portions were processed to assess water content.

qRT-PCR

Total RNA was extracted using TRIzol (Invitrogen) and a Nanodrop spectrophotometer (ND-100; Thermo, Waltham, MA, USA) used to assess resulting RNA concentrations. Total RNA was reverse transcribed to complementary DNA (cDNA) using the HiScript 1st Strand cDNA Synthesis Kit (Vazyme, Nanjing, China) according to the manufacturer's instructions. The stem-loop RT-qPCR method was used to generate cDNA from miRNAs.[18] All qRT-PCR experiments were performed in triplicate using the ABI StepOnePlus™ real-time PCR system (Applied Biosystems, Foster City, CA, USA). The thermocycling program used was as follows: pre-incubation at 95°C for 10 min, 35 cycles of denaturation at 95°C for 15 s, annealing at 60°C for 5 s, and elongation at 72°C for 12 s. Endogenous controls were U6 and β-actin and were used to generate miRNA and messenger RNA (mRNA) expression profiles, respectively. All expression levels were normalized to their respective endogenous control, and the $2^{-\Delta\Delta Ct}$ method[20] was used to calculate fold-change in gene expression. Primers are provided in Table 1.

Western blot analysis

Nuclear, cytoplasmic, and whole protein concentrations obtained from rat pancreatic tissue were determined using the bicinchoninic acid (BCA) method,[22] after which all proteins were run on 10% sodium dodecyl sulfate polyacrylamide gel

Table 1. Primers used for qRT-PCR.

miR-181b	F-5′-ACATTCATTGCTGTCGGTGGGT-3′ R-5′-CGCTTCACGAATTTGCGTGTCA-3′	215 bp
U6	F-5′−GTGCTCGCTTCGGCAGCACATATAC-3′ R-5′-AAAAATATGGAACGCTCACGAATTTG-3′	237 bp
FSTL1mRNA	F-5′-TTATGATGGGCAGGCAAAGAA-3′ R-5′-ACTGCCTTTAGAGAACCAGCC-3′	318 bp
TREM1 mRNA	F-5′-TGGTCTTCTCTGTCCTGTTTG-3′ R-5′-ACTCCCTGCCTTTTACCTC-3′	254 bp
Akt mRNA	F-5′-TCACCTCTGAGACCGACACC-3′ R-5′-ACTGGCTGAGTAGGAGAACTGG-3′	174 bp
β-actin	F-5′-GATTACTGCTCTGGCTCCTGC-3′ R-5′-GACTCATCGTACTCCTGCTTGC-3′	190 bp

qRT-PCR: quantitative real-time polymerase chain reaction

electrophoresis (SDS-PAGE; Bio-Rad, Hercules, CA, USA) using an 80-μg protein aliquot or equal amount of concentrated supernatant, 100 V was used, and for 100 min. The proteins were separated using 4-12% gradient SDS-PAGE and transferred onto polyvinylidene difluoride membranes, 17 mA was used and for overnight. Membranes were blocked with 5% (w/v) milk in TBST (0.05% Tween) at room temperature under agitation for 1 h to prevent non-specific binding. Blots were then incubated overnight at 4°C with primary antibodies including anti-FSTL1 (1:1000), anti-TREM1 (1:1000), anti-Beclin1 (1:200), anti-Akt (1:1000), anti-phospho-Akt (1:1000), anti-TLR4 (1:200), anti-TRAF6 (1:500), anti-IRAK1 (1:500), anti-phospho-IRAK1 (1:500), anti-phospho-p38MAPK (1:1000), anti-p38MAPK (1:1000), anti-NF-kBp65 (1:1000), anti-phospho-NF-kBp65 (1:1000), anti-IκB-a (1:1000), anti-phospho-IκB-a (1:1000), and anti-β-actin (1:1000) diluted in 5% bovine serum albumin (BSA). Lamin-A and β-actin were used as the internal references for nuclear/cytoplasmic and whole proteins, respectively. After overnight incubation, membranes were washed with TBST and incubated for 1 h at room temperature with the appropriate secondary goat anti-rabbit IgG-horseradish peroxidase (HRP) antibody (Santa Cruz Biotechnology, Dallas, TX, USA; 1:2000) or goat anti-mouse IgG-HRP antibody (Santa Cruz Biotechnology; 1:2000). All secondary antibodies were diluted in 5% (w/v) milk in TBST. The same protein load was confirmed with β-actin. All Western blots were densitometrically quantified using the Bio-Rad Universal Hood and Quantity One software (Bio-Rad). All results were normalized to β-actin levels in each lane.

Immunohistochemical analysis

Pancreatic tissue sections were subjected to antigen retrieval with Retrievagen A (Zymed Laboratories, Inc., San Francisco, CA, USA) and endogenous peroxidase activity quenched with 3% H_2O_2 (Tianjin Jinqiang Chemical Co. Ltd., Tianjin, China). Sections were then blocked in 2% BSA in phosphate buffered saline (PBS) to prevent non-specific binding and incubated with primary anti-NF-κB antibody (1:200; BD Pharmingen, Woburn, MA, USA) for 1 h at room temperature. Sections were then washed with PBS and incubated with a biotinylated rabbit anti-goat antibody (Thermo, Freemont, CA, USA) for 30 min at 37°C. Sections were developed using Vectastain ABC and 3,3′-diaminobenzidine (Sigma-Aldrich, St. Louis, MO, USA). Sections were mounted and analyzed: Five fields (magnification, 200×) were randomly selected from each section and the average proportion of NF-κB-positive cells were counted using a true color, multi-functional cell image analysis management system (Image-Pro Plus; Media Cybernetics Inc., Rockville, MD, USA). All results were expressed as positive units (pu).

Myeloperoxidase activity

Pancreatic neutrophil sequestration was quantified by assessing its myeloperoxidase (MPO) activity.[29] Briefly, pancreatic tissue samples were homogenized in 20 mM phosphate buffer (pH 7.4) and centrifuged for 10 min (12,000*g*, 4°C). The pellet was re-suspended in 50 mM phosphate buffer (pH 6) with 0.5% hexadecyltrimethylammonium bromide. The suspensions underwent three cycles of freezing and thawing, sonicated for 60 s, and

Table 2. Acute pancreatitis pathology scoring criteria.

Score	Edema	Inflammation	Necrosis	Hemorrhage
0	Absent	Absent	Absent	Absent
1	Focally increased between lobules	Around ductal margins	Periductal parenchymal destruction	Blood in parenchyma (<25%)
2	Diffusely increased between lobules	In parenchyma (<50% of lobules)	Focal parenchymal necrosis (<20%)	Blood in parenchyma (25%–50%)
3	Tense acini and widely separated lobules	In parenchyma (51%–75% of lobules)	Diffuse loss of lobules (20%–50%)	Blood in parenchyma (50%–75%)
4	Gross lobular separation	Massive collections and abscesses	Severe loss of lobules (>50%)	Blood in 100% of lobules

centrifuged for an additional 5 min (12,000*g*, 4°C). The supernatant was used for MPO assay. A Beckman spectrophotometer (DU640B; Beckman Coulter, CA, USA) was used to detect absorbance changes at 450 nm after 5 min of incubation. One unit of MPO activity (units/milligram of tissue) was defined as the amount required to break down 1 mmol of peroxide per minute at 25°C.

Serum amylase, lipase, TREM1, and pro-inflammatory cytokine levels and levels of DNA-bound NF-KB65 and TLR4 in the pancreas and ileum

Serum activities of amylase and lipase were determined using commercially available kits and in conjunction with a Roche/Hitachi modular analytics system (Roche, Mannheim, Germany). A commercial ELISA kit (Quantikine; R&D Systems, Minneapolis, MN, USA) was used to determine the serum levels of TNF-α, IL-8, ACAM-1, IL-6, IL-12, and TREM1 according to the manufacturer's instructions. Levels of DNA-bound NF-KB65 and TLR4 in pancreas and ileum tissue were also assessed using separate, commercially available ELISA kits according to the manufacturer's instructions.

Serum endotoxin and D-lactate assays

Previously collected blood samples were added in ethylenediaminetetraacetic acid (EDTA)-containing tubes, centrifuged, and the serum isolated. Serum samples were stored at −80°C until later assays. Serum endotoxin levels were determined using a quantitative chromogenic endpoint Limulus Amebocyte Lysate (LAL) QCL-1000 kit (Lonza, Walkersville, MD, USA) according to the manufacturer's instructions. Serum D-lactate levels were spectrophotometrically determined using commercially available kits (Genmed, Shanghai, China) according to the manufacturer's instructions.

Pancreatic water content

Pancreata were weighed to assess changes in pancreatic interstitial edema. To determine pancreatic water content, a fresh pancreas sample was blotted, weighed, dried for 12 h at 95°C, and then weighed again. The difference in weight between wet and dry pancreas was calculated as the tissue wet weight percentage.

Histological examination and scoring of the pancreas

Pancreata were fixed overnight in 10% buffered formalin at 4°C and embedded in paraffin. Full-length (4 μm) sections were acquired and stained with hematoxylin and eosin (H&E) for later histological evaluation. According to previously published methods,[30] edema, hemorrhage, inflammation, and necrosis were graded from 0 to 4 as shown in Table 2.

Histopathological assessment of ileal tissue

After blood sample collection, ileal tissue samples were harvested for later evaluation of any histopathological changes. Briefly, sections were stained with H&E and then examined under light microscopy and blind conditions by two pathologists. Both pathologists assessed ileal histopathology according to the standard scale established by Chiu et al.[31] The degree of mucosal damage was graded as follows: 0 = normal mucosa, 1 = development of subepithelial space at the tip of the villus, 2 = extension of the space with epithelial lifting, 3 = massive epithelial lifting, 4 = denuded villi, and 5 = disintegration of the lamina propria.

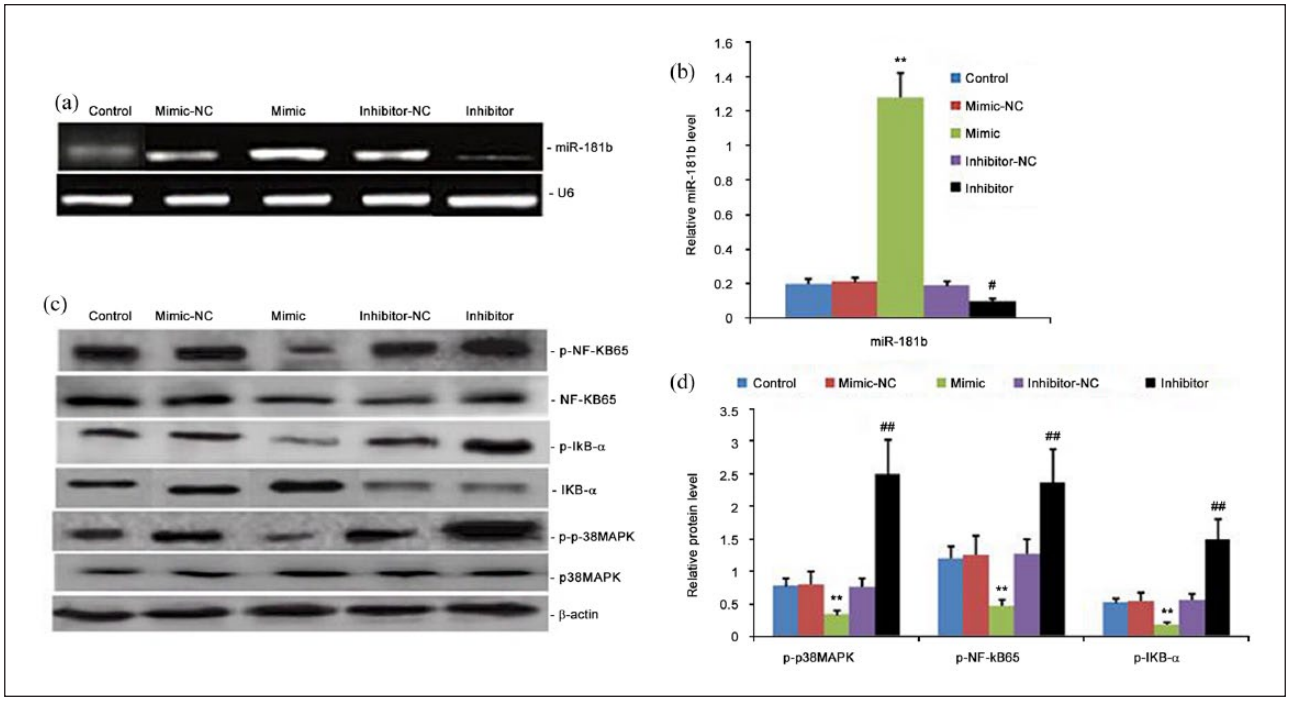

Figure 1. Effect of miR-181b on p38MAPK/NF-κB signaling pathway. (a) and (b) qRT-PCR analysis of miR-181b levels in pancreatic acinar cells transfected with control mimic, miR-181b mimic, control inhibitor, or miR-181b inhibitor. (b) Representative images. (c) and (d) Quantitative Western blot analysis of p38MAPK, p-p38MAPK, NF-κB65, p-NF-κB65, IkB-α, and p-IκB-α protein levels in pancreatic acinar cells transfected with control mimic, miR-181b mimic, control inhibitor, or miR-181b inhibitor. The data are expressed as mean ± SD of three independent experiments. *$P < 0.05$, vs the control group and mimic-NC; #$P < 0.05$, vs inhibitor-NC.

Statistical analyses

All statistical analyses were performed in SPSS 11.0 software (SPSS, Inc., Chicago, IL, USA). Data were expressed as mean ± SD from several independent experiments, as specified in the figure legends. Statistical comparisons between the treatment and control groups were evaluated using a *t*-test. Linear correlational analyses determined the relationship between two variables. Cochran's *Q* test with corresponding analysis of variance (ANOVA) was used to perform multiple comparisons (when greater than three groups). $P < 0.05$ was used to determine statistical significance.

Results

miR-181b significantly downregulated the p38MAPK/NF-κB signaling pathway in pancreatic acinar cells

We first sought to understand the effects of miR-181b on the p38MAPK/NF-κB signaling pathway in pancreatic acinar cells. To do this, miR-181b mimic, miR-181b inhibitor, miR-181b mimic-NC, and miR-181b inhibitor-NC were individually mixed with Lipofectamine 2000 (Invitrogen) to transfect pancreatic acinar cells. At 24 h post-transfection, qRT-PCR was used to measure miR-181b levels and Western blot was used to measure NF-κBp65, p-p38MAPK, and p-IκB-α levels. Results showed that the miR-181b mimic significantly increased miR-181b levels, while the miR-181b inhibitor significantly decreased miR-181b expression (Figure 1(a) and (b)), This decrease in miR-181b levels led to enhanced expression of NF-κBp65, p-IκB-α, and p-p38MAPK; conversely, increasing miR-181b significantly reduced the expressions of NF-κBp65, p-IκB-α, and p-p38MAPK (Figure 1(c) and (d)). These findings suggest that miR-181b may play a role in the regulation of p38MAPK/NF-κB pro-inflammatory signaling pathways.

Overexpression of miR-181b blocked TREM1 and FSTL1 protein levels and ameliorated pancreatic damages in rats with taurocholate-induced SAP

In order to explore the relationship between overexpression of miR-181b and pancreatic damage in rats subjected to taurocholate-induced SAP, an

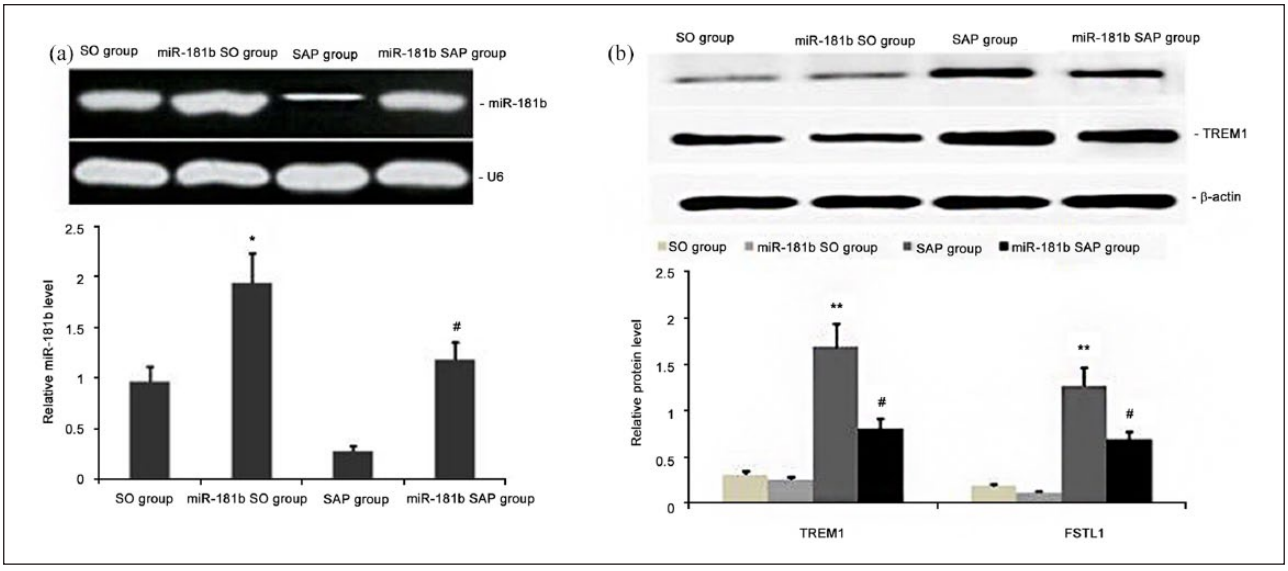

Figure 2. Effect of AdCMV-miR-181b on TREM1 and FSTL1 protein levels. An active miR-181b expression construct (1×109 pfu of AdCMV-miR-181b) was delivered to rats by intravenous tail administration, followed by taurocholate-induced pancreatitis administration over 10 days. TREM1 and FSTL1 protein levels were determined using Western blot and qRT-PCR used to determine miR-181b expression levels. (a) qRT-PCR analysis of miR-181b levels in pancreatic tissue from four experimental groups (SO group, miR-181b SO group, SAP group and miR-181b SAP group). (b) Quantitative Western blot analysis of in pancreatic tissue from four experimental groups (SO group, miR-181b SO group, SAP group and miR-181b SAP group). The data are expressed as mean ± SD of three independent experiments. $^{*}P < 0.05$, $^{**}P < 0.01$, vs the SO group; $^{\#}P < 0.05$, vs the SAP group.

active miR-181b expression construct (1×10^9 pfu of AdCMV-miR-181b) was delivered to rats by tail intravenous administration. After taurocholate-induced pancreatitis was induced over the course of 10 days, pancreatic miR-181b levels were determined using qRT-PCR, while pancreatic TREM1 and FSTL1 protein levels were determined using Western blot. Results indicated that intravenous administration of AdCMV-miR-181b significantly increased miR-181b levels (Figure 2(a)). This administration also significantly blocked pancreatic TREM1 and FSTL1 protein levels (Figure 2(b)). Histopathological examination of the pancreas of taurocholate-treated miR-181b rats revealed the markedly reduced inflammatory cell infiltration, severe edema, and a high degree of destruction of the histoarchitecture of the acini cells when compared with control rats (Figure 3).

FSTL1 and TREM1 are direct targets of miR-181b

We next sought to determine how miR-181b mediated the AP inflammatory response. We used a well-known database to predict likely targets of miR-181b and found FSTL1 and TREM1—both of which are also important pro-inflammatory regulators of AP. Analysis revealed that FSTL1 and TREM1 mRNA and protein levels were dramatically reduced after miR-181b overexpression (Figure 4(a) and (b)). To validate the interaction between miR-181b and these two candidates (FSTL1 and TREM1), we constructed wild-type and mutant FSTL1 and TREM1 for a dual luciferase reporter assay (Figure 4(c) and (d)). As hypothesized, miR-181b bound to the wild-type FSTL1 and TREM1, rather than the mutants (Figure 4(d)).

Effects of Panax notoginseng *saponins on the expressions of miR-181b, FSTL1, Akt, and TREM1 in SAP pancreas*

We next sought to determine the pancreatic mRNA and protein levels of miR-181b, FSTL1, TREM1, and Akt in taurocholate-induced SAP. The levels of miR-181 were significantly reduced, while FSTL1, TREM1, and Akt mRNA levels as well as FSTL1, TREM1, and phosphorylated Akt protein levels were significantly upregulated (Figure 5(a)–(d)). After the administration of *Panax notoginseng* saponins, miR-181b expression was significantly increased. Correspondingly, mRNA levels of

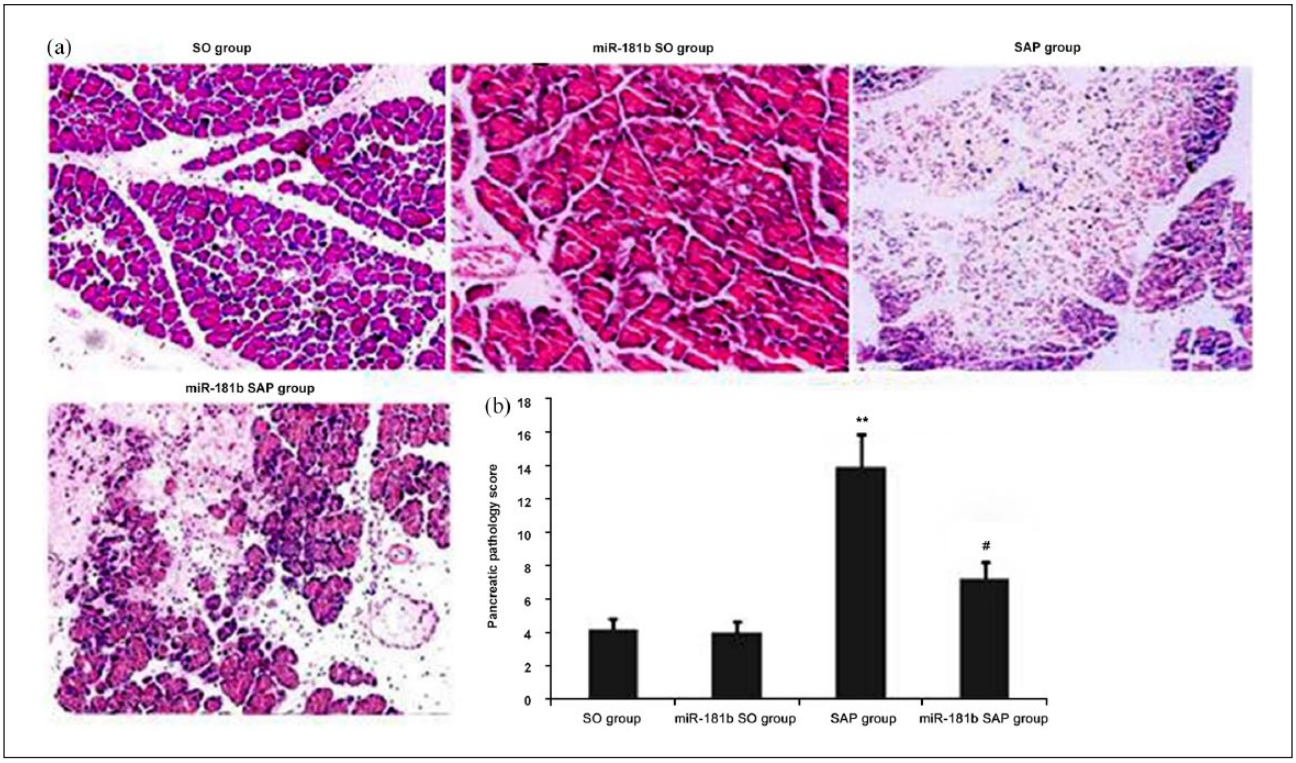

Figure 3. Effect of AdCMV-miR-181b on pancreatic damage. An active miR-181b expression construct (1×109 pfu of AdCMV-miR-181b) was delivered to rats by intravenous tail administration, followed by taurocholate-induced pancreatitis administration over 10 days. (a) Representative images of H&E-stained pancreatic sections from three experimental groups (magnification, 400×). (b) Pancreatic damage score. The data are expressed as mean ± SD of three independent experiments. $^{*}P < 0.05$, $^{**}P < 0.01$, vs the SO group and the miR-181b SO group; $^{\#}P < 0.05$, vs the SAP group.

FSTL1, TREM1, and Akt as well as the protein levels of FSTL1, TREM1, and phosphorylated Akt were all significantly reduced (Figure 5(a)–(d)). In sum, *Panax notoginseng* saponins suppressed mRNA and protein levels of FSTL1, TREM1, and Akt, but upregulated miR-181b expression.

Effects of Panax notoginseng *saponins on pancreatic protein levels of TLR4, p-IκB-α, TRAF6, p-IRAK1, p-p38MAPK, and p-NF-κBp65 in taurocholate-induced SAP*

We next determined the effects of *Panax notoginseng* saponins on pancreatic protein levels of TLR4, TRAF6, p-p38MAPK, p-IRAK1, p-IκB-α, and p-NF-κBp65 in rats treated with taurocholate using Western blot. In vivo pancreatic protein levels of TLR4, p-IRAK1, TRAF6, p-NF-κBp65, p-p38MAPK, and p-IκB-α were significantly increased in taurocholate-induced SAP group ($P < 0.05$; Figure 6). Interestingly, these levels were significantly reduced after *Panax notoginseng* saponin administration ($P < 0.05$; Figure 6).

Panax notoginseng *saponins inhibited NF-κBp65 activity in rat pancreas and ileum tissues with taurocholate-induced SAP*

To explore the effects of *Panax notoginseng* saponins on NF-κBp65 activation in taurocholate-induced SAP, pancreatic and ileal tissue sections were subjected to immunohistochemical staining. NF-κBp65 expression was weak in both the SO and treatment SO groups (Figure 7(a)–(d)). However, NF-κBp65 expression was significantly increased ($P < 0.05$) in the taurocholate-induced AP group. However, 24 h after *Panax notoginseng* saponin administration, NF-κBp65 activity in the pancreas and ileum of taurocholate-induced SAP rats was blocked ($P < 0.05$; Figure 7(a)–(d)).

Panax notoginseng *saponins inhibited pancreatic and ileal DNA-bound NF-KB65 and TLR4 in taurocholate-induced SAP*

To analyze the effects of *Panax notoginseng* saponins on DNA-bound NF-KB65 and TLR4 in

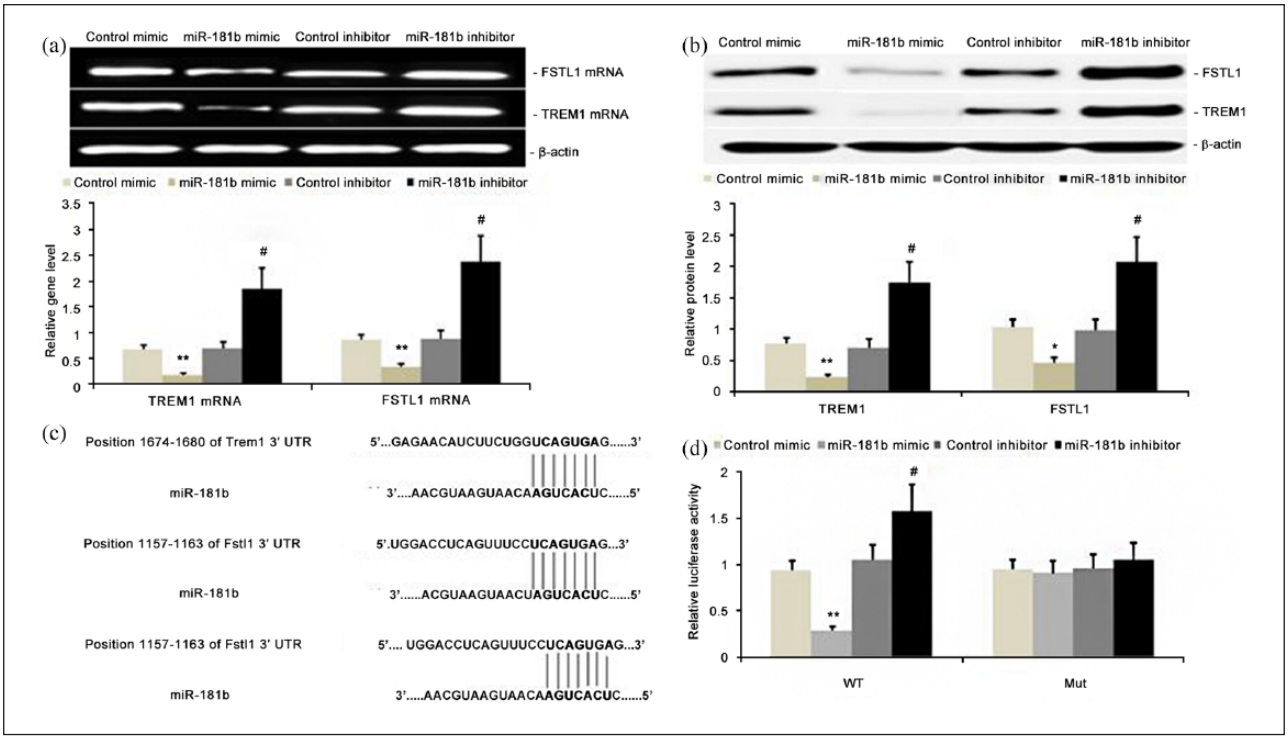

Figure 4. FSTL1 and TREM1 are two downstream targets of miR-181b. (a) Reduced mRNA levels of FSTL1 and TREM1 in pancreatic acinar cells after miR-181b overexpression ($P < 0.05$); levels were enhanced after miR-181b downregulation ($P < 0.05$). (b) FSTL1 and TREM1 were decreased in cells with miR-181b overexpression when compared with empty vector control ($P < 0.05$). FSTL1 and TREM1 were significantly increased in cells with miR-181b downregulation. (c) miR-181b bound to the 3′-UTR regions of FSTL1 and TREM1, and binding was interrupted in mutant FSTL1 and TREM1. (d) Dual luciferase reporter assay indicated that miR-181b mimic bound to the 3′-UTR region of wild-type FSTL1 and TREM1, rather than FSTL1 and TREM1 mutants ($P < 0.05$).

taurocholate-induced SAP, nuclear protein from tissue sections of the pancreas and ileum were isolated using NE-PER Nuclear and Cytoplasmic Extraction Reagents (Pierce, Waltham, MA, USA). DNA-bound NF-KB65 and TLR4 were then measured using ELISA. DNA-bound NF-KB65 and TLR4 were markedly decreased in the SO group (Figure 7(e)–(h)). However, DNA-bound NF-KB65 and TLR4 were significantly increased ($P < 0.05$) in the taurocholate-induced AP group. Notably, 24 h after *Panax notoginseng* saponin administration, DNA-bound NF-KB65 and TLR4 in the pancreas and ileum of taurocholate-induced SAP rats were attenuated ($P < 0.05$; Figure 7(e)–(h)).

Effects of Panax notoginseng *saponins on MPO activity in the pancreata of rats with taurocholate-induced SAP*

After taurocholate induction of SAP, pancreatic MPO activity was significantly increased. However, administration of *Panax notoginseng* saponins resulted in a significant reduction in MPO activity (Figure 8(b)).

Effects of Panax notoginseng *saponins on serum levels of TREM1, TNF-α, ICAM-1, IL-6, and IL-12*

Serum levels of the pro-inflammatory cytokines (TNF-α, ICAM-1, IL-6, and IL-12) and pro-inflammatory protein (TREM1) were significantly increased in taurocholate-induced SAP rats. However, administration of *Panax notoginseng* saponins resulted in significant reductions in the levels of TREM1, TNF-α, ICAM-1, IL-6, and IL-12 (Figure 8(a), (c)–(f)).

Effects of Panax notoginseng *saponins on the ratio of the pancreas to body weight, ascites, and serum amylase activity in taurocholate-induced SAP rats*

Pancreatic edema is a major assessment criterion of pancreatitis; given this, we sought to determine

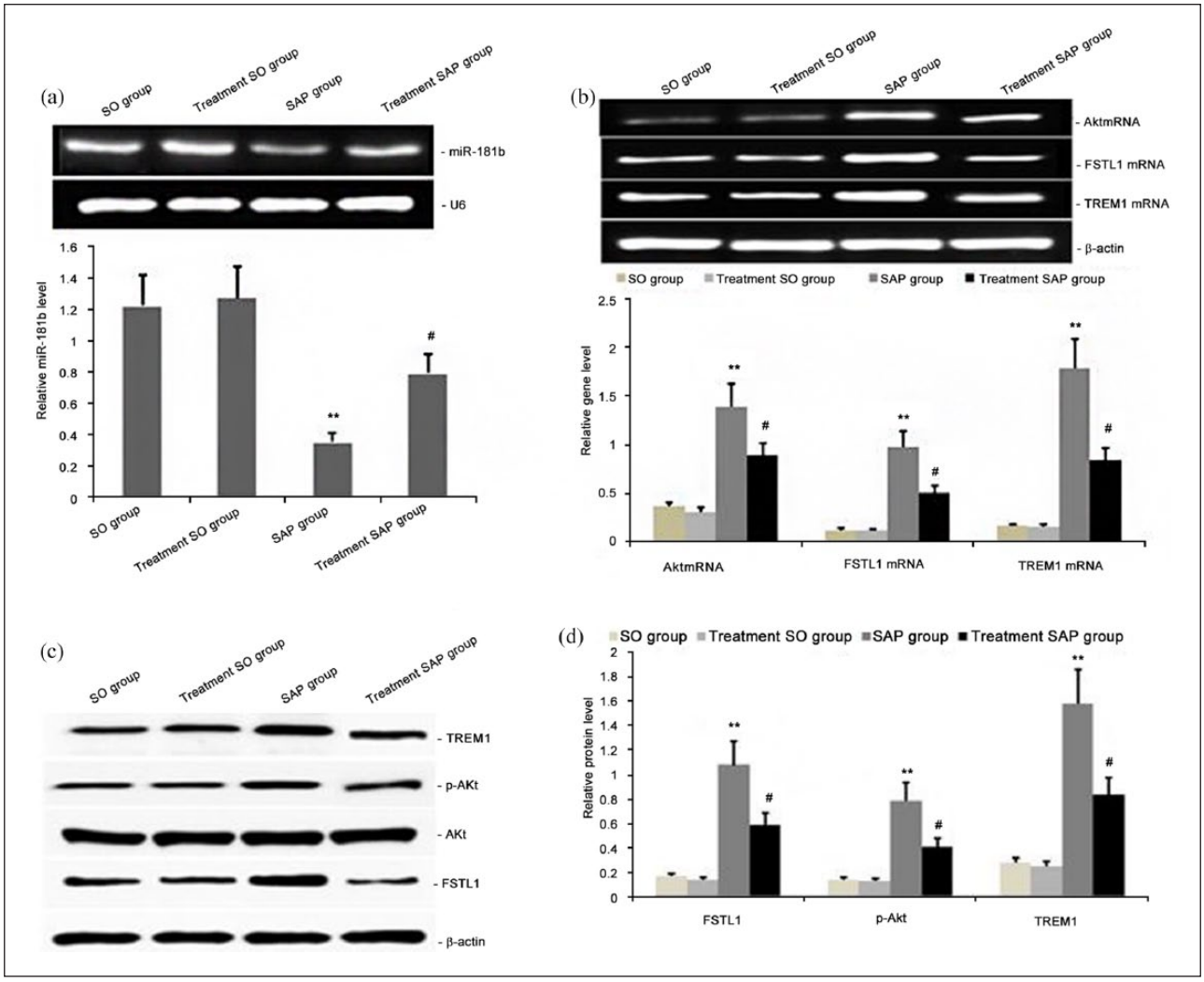

Figure 5. Effect of miR-181b upregulation by *Panax notoginseng* saponins on FSTL1, Akt, and TREM1 gene and protein levels and other pro-inflammatory proteins in the pancreas of SAP rats. (a) Effect of *Panax notoginseng* saponins on miR-181b levels. Pancreatic miR-181b levels were determined using qRT-PCR. (b) Effect of *Panax notoginseng* saponins on FSTL1, Akt, and TREM1 gene levels. Pancreatic levels of FSTL1, Akt, and TREM1 genes were determined using qRT-PCR. (c) Representative Western blots indicating pancreatic levels of FSTL1, Akt, p-Akt, and TREM1 24 h after administration of *Panax notoginseng* saponins. (d) Statistical summary of the densitometric analysis of FSTL1, p-Akt, and TREM1 expression. The data are expressed as mean ± SD of three independent experiments. $^{**}P < 0.01$, vs the SO group and the treatment SO group; $^{\#}P < 0.05$, vs the SAP group.

if there was any difference after treatment with *Panax notoginseng* saponins. After 5% sodium taurocholate was injected into the biliary-pancreatic duct of rats, the ratios of the pancreas to body weight and ascites were significantly increased (Figure 9(a)–(c)). In addition, serum amylase was significantly increased in SAP rats. However, *Panax notoginseng* saponin treatment significantly reduced serum amylase activity. It also significantly reduced ascites and the ratio of the pancreas to body weight, indicating a beneficial effect of *Panax notoginseng* saponins on pancreatic edema and injury (Figure 9(a)–(c)).

Effects of Panax notoginseng *saponins on serum endotoxin and* D*-lactate in taurocholate-induced SAP rats*

Serum levels of endotoxin, D-lactate, and TREM1 were also measured to analyze the effects of *Panax notoginseng* saponins in SAP rats. Serum endotoxin and D-lactate levels were significantly increased 24 h after the administration of 5% sodium taurocholate (Figure 9(d) and (e)). However, *Panax notoginseng* saponin treatment significantly reduced serum levels of both endotoxin and D-lactate.

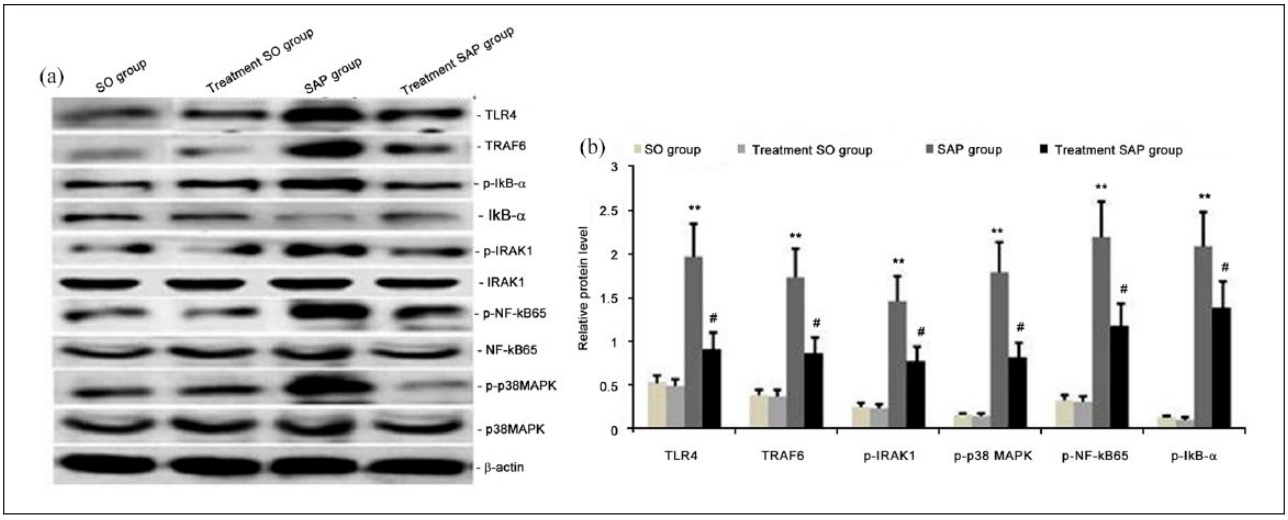

Figure 6. Effect of *Panax notoginseng* saponins on TLR4, IRAK1, TRAF6, NF-κBp65, p-p38MAPK, and P-IκB-α protein expression in the pancreas of rats with taurocholate-induced SAP. (a) Representative graphs of TLR4, IRAK1, p-IRAK1, TRAF6, NF-κBp65, p-NF-κBp65, p38MAPK, p-p38MAPK, and P-IκB-α protein levels 24 h after administration of *Panax notoginseng* saponins. (b) Statistical analysis of protein levels of FSTL1, Akt, p-Akt, TREM1, TLR4, p-IRAK1, TRAF6, p-NF-κBp65, p-p38MAPK, and P-IκB-α. The data are expressed as mean ± SD of three independent experiments. $^{**}P < 0.01$, vs the SO group and the treatment SO group; $^{\#}P < 0.05$, vs the SAP group.

Effects of Panax notoginseng *saponins on pancreatic and ileal histology in taurocholate-induced SAP rats*

In order to evaluate the effects of *Panax notoginseng* saponins on local pancreatic and ileal injury, we next examined pancreatic and ileal morphology. The SAP group showed a high degree of destruction of the histoarchitecture of acini cells, severe edema, and significantly higher pancreatic pathological scores than those in either the SO or treatment SO groups (Figure 9(f)–(h)). After SAP induction of SAP, villi and crypt structures were also partially damaged; in particular, hair became thinner and shorter. We also observed heavy inflammatory cell infiltration in the intrinsic membrane as well as lymphatic dilatation and edema (Figure 9(h) and (i)). In the *Panax notoginseng* saponin treatment group, injuries to the pancreatic and ileal tissues were alleviated, with significant reductions in pancreatic and ileal injury scores (Figure 9(f)–(i)).

Discussion

The initial and subsequent rapid deterioration in SAP may be caused by the overexpression of pro-inflammatory cytokines, which are believed to be critical to the pathogenesis of the disease.[1] In particular, cytokines from macrophages are considered to play an integral role in the development of AP.[3] In this study, taurocholate-induced SAP led to increased levels of TNF-α, ACAM-1, IL-6, IL-12, and IL-8; critically, *Panax notoginseng* saponin treatment significantly reduced levels of TNF-α, ACAM-1, IL-6, IL-12, and IL-8. These results were consistent with our pancreatic MPO activity analysis, indicating neutrophil and macrophage diapedesis[32] in the pancreas. *Panax notoginseng* saponins successfully attenuated pancreas' MPO activity, blocked tissue neutrophilia, and ameliorated taurocholate-induced pancreatic injury.

To explore the effects of miR-181b on SAP, we measured miR-181b expression in rat pancreatic tissue. Pancreatic miR-181b levels were significantly downregulated in pancreatic tissue samples from rats with SAP. Moreover, the level of downregulation was associated with an exacerbated pancreatitis response and worse pancreatic injury. However, miR-181b overexpression attenuated the pancreatitis response and ameliorated pancreatic injury, highlighting the key role miRNAs play as post-transcriptional regulators of biological processes.[17,18,33] Key inflammatory regulators are related to the homeostatic response to inflammatory stimuli by activating the TLR4 pathway[34] and various TLR-mediated immune responses to bacterial infection by either suppressing the

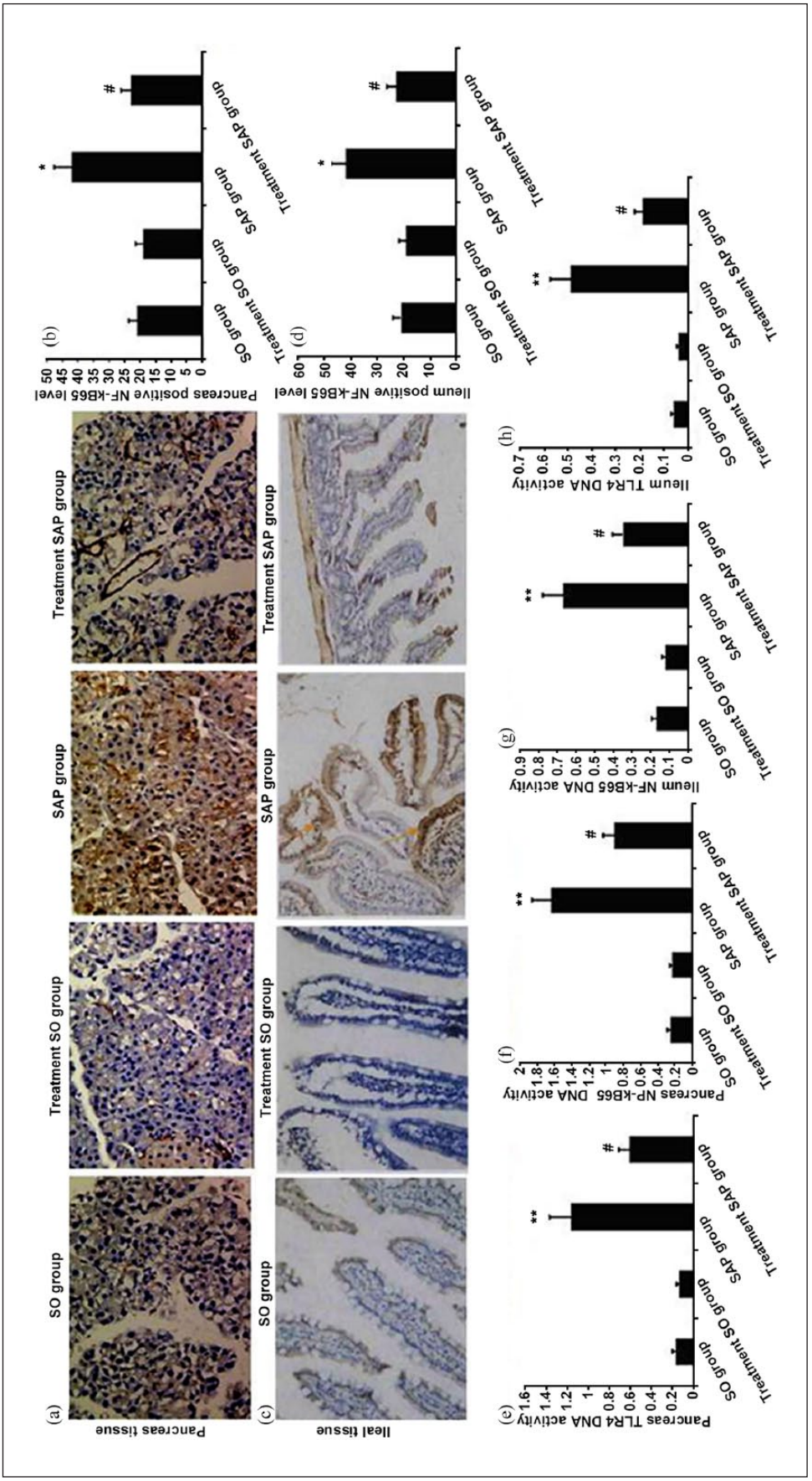

Figure 7. *Panax notoginseng* saponins attenuated the DNA binding of NF-κBp65, NF-KB65, and TLR4 in pancreatic and ileal tissue of rats with taurocholate-induced SAP. (a) and (c) Representative graphs of NF-κB65-positive expression in pancreatic and ileal tissue. (b) and (d) Statistical analysis of NF-κB65-positive expression in pancreatic and ileal tissue. (e)–(h): DNA binding of NF-KB65 and TLR4 in rat pancreas and ileum as determined by ELISA. The data are expressed as mean ± SD of three independent experiments. $^{*}P < 0.05$, $^{**}P < 0.01$, vs the SO group and the treatment SO group; $^{\#}P < 0.05$, $^{\#\#}P < 0.01$, vs the SAP group.

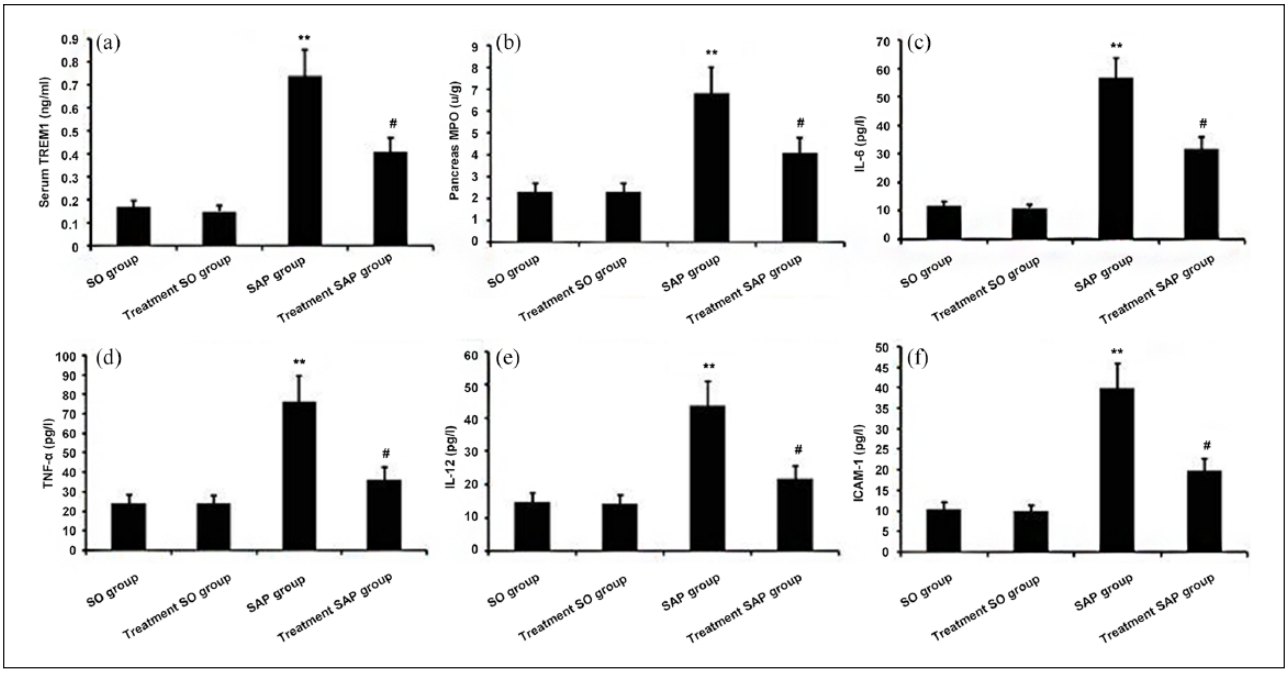

Figure 8. *Panax notoginseng* saponins attenuated the pancreatic inflammatory response. Two hours before taurocholate-induced SAP, rats in the treatment group received *Panax notoginseng* saponin extract (50 mg/kg) via tail intravenous injection every 8 h for 24 h. After 24 h, MPO activity was measured using a commercially available MPO kit, and serum levels of TREM1, TNF-α, ICAM-1, IL-6, and IL-12 were measured by ELISA. (a) Serum TREM1 levels. (b) Pancreas MPO activity levels; (c) serum levels of IL-6. (d) serum levels ofTNF-α. (e) serum levels of IL-12. (f) serum levels ofand ICAM-1. The data are expressed as mean ± SD of three independent experiments. $^{**}P < 0.01$, vs the SO group and the treatment SO group; $^{\#}P < 0.05$, vs the SAP group.

inflammatory response or reducing inflammatory triggers.[35] The miR-181 family may control inflammation under pathological conditions, thus affecting growth, activation, and development.[36] The results presented here were consistent with previous work.[37] To this end, there is evidence that miR-181a, miR-181b, and miR-181d function as regulators of TLR/NF-κB signaling as their expression is significantly decreased in the monocytes of obese patients. Correspondingly, their levels were increased and restored to the normal levels in lean subjects who had lost weight.[38] Moreover, type 2 diabetes patients administered resveratrol-enriched grape extracts for 1 year had decreased expression of pro-inflammatory cytokines—including CCL3, TNF-α, and IL-1β—in peripheral blood mononuclear cells. This was also associated with increased expression of six miRNAs, including miR-181b.[39] Thus, the correlation results combined with the known role of miR-181b in reducing downstream NF-κB signaling[37] suggest that miR-181b plays a protective role in inflammatory diseases.

Emerging evidence strongly indicates a role for TREM1 in non-infectious inflammatory disorders.[40] TREM1 possesses the ability to amplify signaling in either a TLR4- or TLR2-dependent manner.[41] In particular, the co-stimulation of neutrophils or monocytes with the TLR4 ligand and endotoxin LPS results in a synergistic increase in pro-inflammatory cytokine expression.[41,42] Our study found that TREM1 was the direct target of miR-181b. The decrease in miR-181b by taurocholate-induced AP significantly increased TREM1 levels. This significant increase was correlated with increased activities of TLR4 and the p38 MAPK signaling pathway, as well as worse taurocholate-induced pancreatic injury. Our study also found that this increase in TREM1 level was inhibited by upregulation of miR-181b after *Panax notoginseng* saponin administration. This inhibitory effect was correlated with the reduced activities of TLR4 and the p38 MAPK signaling pathway, as well as improved taurocholate-induced pancreatic damage.

Our results clearly showed that *Panax notoginseng* saponins inhibited the IRAK1/TRAF6 signaling pathway and reduced pancreatic inflammation. Specifically, IRAK1 is an adaptor for the Toll/IL-1R receptor signaling complex.[43] IRAK4 may also

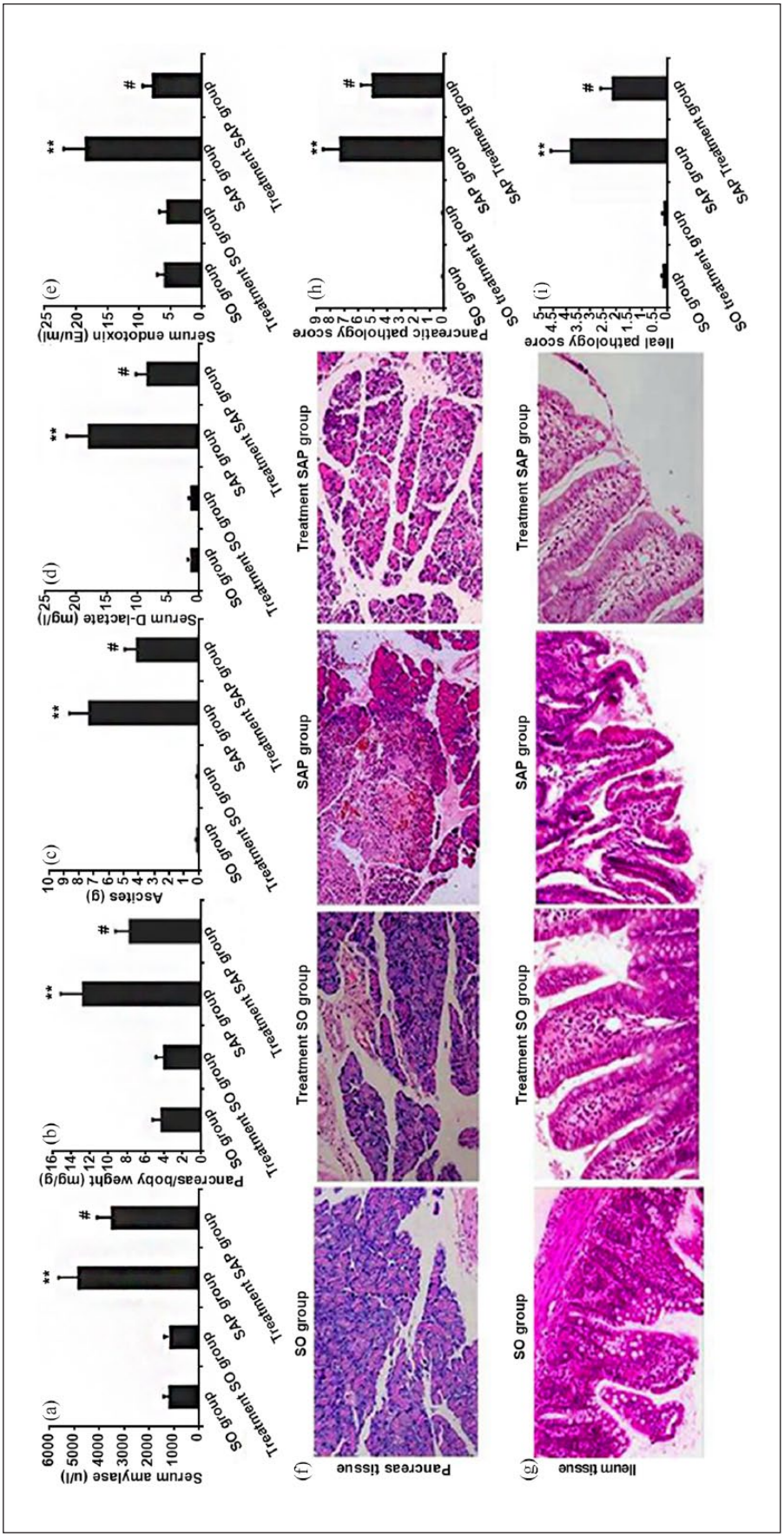

Figure 9. *Panax notoginseng* saponins ameliorated pancreatic and ileal tissue injuries. Two hours before taurocholate-induced SAP, rats in the treatment group received *Panax notoginseng* saponin extracts (50 mg/kg) via tail intravenous injection every 8 h for 24 h (three injections total). (a)–(e): Quantitative analysis of the ratio of the pancreas to body weight, serum amylase activity, ascites, serum endotoxin, and D-lactate after 24 h. (f) and (g) Representative images of H&E-stained pancreatic and ileal sections from five experimental groups (magnification, 400×). (h)–(i) Representative statistical analysis of pancreatic and ileal pathological scores. The data are expressed as mean ± SD of three independent experiments. $^{*}P < 0.05$, $^{**}P < 0.01$, vs the SO group and the treatment SO group; $^{\#}P < 0.05$, $^{\#\#}P < 0.01$, vs the SAP group.

phosphorylate IRAK1 to initiate its autophosphorylation. Hyperphosphorylated IRAK1 dissociates from the complex, dimerizes, and is bound to TNF receptor–associated factor 6 (TRAF6). IRAK1 binds to TRAF6 with Ubc13/Uev1A to catalyze the Lys63-mediated polyubiquitination of IRAK1. IRAK1 results in the polyubiquitination and dimerization of TRAF6 and thus transforming growth factor-β-activated kinase 1 (TAK1).[43] TAK1 phosphorylates a suite of regulatory kinases across various signaling pathways, generating and releasing multiple cytokines via NF-κB activation.[44] Finally, activated NF-κB can translocate to the nucleus and bind to promoters of pro-inflammatory genes, thus enhancing the inflammatory response.[44]

NF-κB activation can lead to other signaling pathways, such as TLR and p38MAPK, which have been extensively explored.[44] Inhibitors of p38MAPK (SB203580) can decrease the levels of LPS-induced pro-inflammatory proteins.[45] Here, *Panax notoginseng* saponins reduced p38 MAPK and NF-κB signaling activity, DNA-bound NF-KB65 and TLR4 in the pancreas and ileum of taurocholate-induced SAP rats, and pancreas and ileum inflammation. *Panax notoginseng* saponin treatment also attenuated taurocholate-induced pancreatic damage.

FSTL1 significantly promotes the expression of inflammatory cytokines by activating the NF-κB pathway;[46] FSTL1 also activates TLR4 signaling.[47] Here, FSTL1 was shown to be a direct target of miR-181b. Taurocholate-induced AP attenuated the activity of miR-181b, elevated FSTL1 expression, enhanced the activities of TLR4 and MAPK signaling, stimulated the pancreatic inflammatory response, and promoted taurocholate-induced pancreatic damage. Conversely, *Panax notoginseng* saponins enhanced miR-181b expression, blocked FSTL1 expression, attenuated the pancreatic inflammatory response, and reduced taurocholate-induced pancreatic damage.

The PI3K/Akt pathway was identified as an endogenous feedback mechanism for the activation of pro-inflammatory factors.[48,49] Accordingly, PI3K/Akt inhibition is known to decrease serum cytokine levels in mice.[50] Previous studies indicated that Akt could phosphorylate and activate IκB kinase IKK-α and cause the degradation of IκB nuclear translocation of NF-κB. Akt has also been shown to promote cytokine expression, including IL-1β, IL-18, and TNF-α, leading to accelerated inflammation.[9] Here, taurocholate-induced acute pancreatitis downregulated miR-181b activity, stimulated Akt gene expression and phosphorylated Akt expression, and promoted inflammatory gene and protein expression. Collectively, this led to enhanced pancreatic inflammation. However, *Panax notoginseng* saponin administration reduced phosphorylated Akt expression by enhancing miR-181b expression, thus attenuating pancreatic inflammation.

Pancreatic edema is one of the main indicators used for assessing pancreatitis.[3] Serum amylase activity is also a common indicator for assessing pancreatitis.[2] This study confirmed that the administration of *Panax notoginseng* saponins reduced serum amylase activity, attenuated pancreatic edema, and reduced acute pancreatic injury.

AP is often accompanied by intestinal injury.[51] To this end, plasma D-lactic acid is an important indicator to evaluate intestinal mucosal barrier damage.[51] Our data showed that SAP increased serum D-lactic acid levels, confirming the presence of intestinal mucosal barrier damage. This mucosal barrier damage increased intestinal permeability, enhanced serum endotoxin levels, increased pancreatic and intestinal inflammation, and led to more severe SAP. However, in our study, we found that the administration of *Panax notoginseng* saponins ameliorated mucosal barrier damage, blocked intestinal permeability, reduced serum endotoxin levels, attenuated pancreatic and intestinal inflammation, and ameliorated SAP.

Panax notoginseng saponins exert a protective effect against SAP induced by taurocholate. This therapeutic effect is mediated through miR-181b upregulation and inhibition of TREM1, FSTL1, TLR4, NF-κB, and p38 MAPK pathways. This results in reduced pancreatic and intestinal inflammation, ameliorated mucosal barrier damage, decreased serum endotoxin levels, and attenuated taurocholate-induced pancreatic damage. Collectively, our results suggest the potential use of *Panax notoginseng* saponins in the treatment of inflammatory diseases such as AP, sepsis, and MODS.

Acknowledgements

M.-w.L., Y.-q.H., T.-w.F., D.-y.T., Y.-q.W., and M.-x.S conceived and designed the experiments. T.-w.F., D.-y.T., and M.-x.S. conducted the experiments. M.-w.L., D.-m.W., Y.-q.H., and T.-w.F. analyzed all experimental data. M.-w.L, D.-m.W., D.-y.T., and T.-w.F. contributed

reagents and experimental materials as well as tools used for analysis. M.-w.L., D.-y.T., Y.-q.W., and Y.-q.H. wrote the manuscript. All authors have read and approved of the final manuscript. M.-w.L., Y.-q.H. and Y.-p.Q. contributed equally to this work.

Data availability statement

All data obtained for this study are included in the manuscript.

Declaration of conflicting interests

The author(s) declared no potential conflicts of interest with respect to the research, authorship, and/or publication of this article.

Ethics approval

All animal experiments were approved by the Animal Experimental Ethics Committee of Kunming Medical University and performed according to institutional guidelines and ethics.

Funding

The author(s) disclosed receipt of the following financial support for the research, authorship and/or publication of this article: This work was financially supported by Yunnan Applied Basic Research Project-Union Foundation of China (Grant No. 2017FE468(-032)). We thank Cheng Mei She for his technical support.

References

1. John BJ, Sambandam S, Garg P, et al. (2017) Persistent systemic inflammatory response syndrome predicts the need for tertiary care in acute pancreatitis. *Acta Gastro-Enterologica Belgica* 80(3): 377–380.
2. Pan LL, Li J, Shamoon M, et al. (2017) Recent advances on nutrition in treatment of acute pancreatitis. *Frontiers in Immunology* 8: 762.
3. Tenner S, Sica G, Hughes M, et al. (1997) Relationship of necrosis to organ failure in severe acute pancreatitis. *Gastroenterology* 113: 899–903.
4. Thandassery RB, Choudhary N, Bahl A, et al. (2017) Characterization of cardiac dysfunction by echocardiography in early severe acute pancreatitis. *Pancreas* 46(5): 626–630.
5. Mitchell RM, Byrne MF and Baillie J (2003) Pancreatitis. *The Lancet* 361: 1447–1455.
6. Rijkers AP and van Eijck CH (2017) Acute pancreatitis. *The New England Journal of Medicine* 376(6): 596–597.
7. Wang CZ, McEntee E, Wicks S, et al. (2006) Phytochemical and analytical studies of *Panax notoginseng* (Burk.) F.H. Chen. *Journal of Natural Medicines* 60: 97–106.
8. Sun J, Sun G, Meng X, et al. (2013) Ginsenoside RK3 prevents hypoxia-reoxygenation induced apoptosis in H9c2 cardiomyocytes via AKT and MAPK pathway. *Evidence-Based Complementary and Alternative Medicine* 2013: 690190.
9. Yu S, Zhou X, Li F, et al. (2017) Microbial transformation of ginsenoside Rb1, Re and Rg1 and its contribution to the improved anti-inflammatory activity of ginseng. *Scientific Reports* 7(1): 138.
10. Lee YJ, Jin YR, Lim WC, et al. (2003) Ginsenoside-Rb1 acts as a weak phytoestrogen in MCF-7 human breast cancer cells. *Archives of Pharmacal Research* 26: 58–63.
11. Korivi M, Hou CW, Huang CY, et al. (2012) Ginsenoside-Rg1 protects the liver against exhaustive exercise-induced oxidative stress in rats. *Evidence-Based Complementary and Alternative Medicine* 2012: 932165.
12. Zhang G, Liu A, Zhou Y, et al. (2008) Panax ginseng-ginsenoside-Rg2 protects memory impairment via anti-apoptosis in a rat model with vascular dementia. *Journal of Ethnopharmacology* 115: 441–448.
13. Wan JB, Lee SM, Wang JD, et al. (2009) Panax notoginseng reduces atherosclerotic lesions in ApoE-deficient mice and inhibits TNF-alpha-induced endothelial adhesion molecule expression and monocyte adhesion. *Journal of Agricultural and Food Chemistry* 57: 6692–6697.
14. Yan YT, Li SD, Li C, et al. (2018) Panax notoginsenoside saponins Rb1 regulates the expressions of Akt/mTOR/PTEN signals in the hippocampus after focal cerebral ischemia in rats. *Behavioural Brain Research* 345: 83–92.
15. Leung KW, Pon YL, Wong RN, et al. (2006) Ginsenoside-Rg1 induces vascular endothelial growth factor expression through the glucocorticoid receptor-related phosphatidylinositol 3-kinase/Akt and beta-catenin/T-cell factor-dependent pathway in human endothelial cells. *Journal of Biological Chemistry* 281(47): 36280–36288.
16. Kura B, Babal P and Slezak J (2017) Implication of microRNAs in the development and potential treatment of radiation-induced heart disease. *Canadian Journal of Physiology and Pharmacology* 95(10): 1236–1244.
17. Esquela-Kerscher A and Slack FJ (2006) Oncomirs—microRNAs with a role in cancer. *Nature Reviews Cancer* 6: 259–269.
18. Sheedy FJ and O'Neill LA (2008) Adding fuel to fire: MicroRNAs as a new class of mediators of inflammation. *Annals of the Rheumatic Diseases* 67(Suppl 3): iii50–iii55.
19. O'Connell RM, Chaudhuri AA, Rao DS, et al. (2010) MicroRNAs enriched in hematopoietic stem cells differentially regulate long-term hematopoietic output.

Proceedings of the National Academy of Sciences of the United States of America 107: 14235–14240.
20. Hatley ME, Patrick DM, Garcia MR, et al. (2010) Modulation of K-Ras-dependent lung tumorigenesis by MicroRNA-21. *Cancer Cell* 18: 282–293.
21. Pichiorri F, Suh SS, Rocci A, et al. (2010) Downregulation of p53-inducible microRNAs 192, 194 and 215 impairs the p53/MDM2 autoregulatory loop in multiple myeloma development. *Cancer Cell* 18: 367–381.
22. Mattiotti A, Prakash S, Barnett P, et al. (2018) Follistatin-like 1 in development and human diseases. *Cellular and Molecular Life Sciences* 75(13): 2339–2354.
23. Chaly Y, Fu Y, Marinov A, et al. (2014) Follistatin-like protein 1 enhances NLRP3 inflammasome-mediated IL-1β secretion from monocytes and macrophages. *European Journal of Immunology* 44(5): 1467–1479.
24. Thankam FG, Roesch ZK, Dilisio MF, et al. (2018) Association of inflammatory responses and ECM disorganization with HMGB1 upregulation and NLRP3 inflammasome activation in the injured rotator cuff tendon. *Scientific Reports* 8(1): 8918.
25. Wu TY, Khor TO, Saw CL, et al. (2011) Anti-inflammatory/anti-oxidative stress activities and differential regulation of Nrf2-mediated genes by non-polar fractions of tea Chrysanthemum zawadskii and licorice Glycyrrhiza uralensis. *American Association of Pharmaceutical Scientists* 13: 1–13.
26. Yu JH, Lim JW, Namkung W, et al. (2002) Suppression of cerulein-induced cytokine expression by antioxidants in pancreatic acinar cells. *Laboratory Investigation* 82(10): 1359–1368.
27. Wu L, Matherly J, Smallwood A, et al. (2001) Chimeric PSA enhancers exhibit augmented activity in prostate cancer gene therapy vectors. *Gene Therapy Journal* 8(18): 1416–1426.
28. Liu MW, Wei R, Su MX, et al. (2018) Effects of Panax notoginseng saponins on severe acute pancreatitis through the regulation of mTOR/Akt and caspase-3 signaling pathway by upregulating miR-181b expression in rats. *BMC Complementary and Alternative Medicine* 18(1): 51.
29. Franck T, Minguet G, Delporte C, et al. (2015) An immunological method to combine the measurement of active and total myeloperoxidase on the same biological fluid, and its application in finding inhibitors which interact directly with the enzyme. *Free Radical Research* 49(6): 790–799.
30. Rongione AJ, Kusske AM, Kwan K, et al. (1997) Interleukin 10 reduces the severity of acute pancreatitis in rats. *Gastroenterology* 112: 960–967.
31. Chiu CJ, Scott HJ and Gurd FN (1970) Intestinal mucosal lesion in low-flow states. II. The protective effect of intraluminal glucose as energy substrate. *Archives of Surgery* 101(4): 484–488.
32. Chen X, Li SL, Wu T, et al. (2008) Proteasome inhibitor ameliorates severe acute pancreatitis and associated lung injury of rats. *World Journal of Gastroenterology*, 14(20): 3249–3253.
33. Quinn EM, Wang J and Redmond HP (2012) The emerging role of microRNA in regulation of endotoxin tolerance. *Journal of Leukocyte Biology* 91: 721–727.
34. Aslam R, Speck ER, Kim M, et al. (2006) Platelet Toll-like receptor expression modulates lipopolysaccharide-induced thrombocytopenia and tumor necrosis factor-alpha production in vivo. *Blood* 107: 637–641.
35. Galicia JC, Naqvi AR, Ko CC, et al. (2014) MiRNA-181a regulates Toll-like receptor agonist-induced inflammatory response in human fibroblasts. *Genes and Immunity* 15(5): 333–337.
36. Sun X, Sit A and Feinberg MW (2014) Role of miR-181 family in regulating vascular inflammation and immunity. *Trends in Cardiovascular Medicine* 24(3): 105–112.
37. Sun X, Icli B, Wara AK, et al. (2012) MicroRNA-181b regulates NF-kappaB-mediated vascular inflammation. *Journal of Clinical Investigation* 122: 1973–1990.
38. Hulsmans M, Sinnaeve P, Van der Schueren B, et al. (2012) Decreased miR-181a expression in monocytes of obese patients is associated with the occurrence of metabolic syndrome and coronary artery disease. *Journal of Clinical Endocrinology and Metabolism* 97(7): E1213–E1218.
39. Tomé-Carneiro J, Larrosa M, Yáñez-Gascón MJ, et al. (2013) One-year supplementation with a grape extract containing resveratrol modulates inflammatory-related microRNAs and cytokines expression in peripheral blood mononuclear cells of type 2 diabetes and hypertensive patients with coronary artery disease. *Pharmacological Research* 72: 69–82.
40. Bleharski JR, Kiessler V, Buonsanti C, et al. (2003) A role for triggering receptor expressed on myeloid cells-1 in host defense during the early-induced and adaptive phases of the immune response. *Journal of Immunology* 170: 3812–3818.
41. Bouchon A, Dietrich J and Colonna M (2000) Cutting edge: Inflammatory responses can be triggered by TREM-1, a novel receptor expressed on neutrophils and monocytes. *Journal of Immunology* 164: 4991–4995.
42. Owens R, Grabert K, Davies CL, et al. (2017) Corrigendum: Divergent neuroinflammatory regulation of microglial TREM expression and involvement of NF-κB. *Frontiers in Cellular Neuroscience* 11: 256.
43. Burns K, Janssens S, Brissoni B, et al. (2003) Inhibition of interleukin 1 receptor/toll-like receptor signaling through the alternatively spliced, short

form of MyD88 is due to its failure to recruit IRAK-4. *Journal of Experimental Medicine* 197: 263–268.
44. Liu MW, Wang YH, Qian CY, et al. (2014) Xuebijing exerts protective effects on lung permeability leakage and lung injury by upregulating Toll-interacting protein expression in rats with sepsis. *International Journal of Molecular Medicine* 34(6): 1492–1504.
45. Liu MW, Su MX, Zhang W, et al. (2014) Protective effect of Xuebijing injection on paraquat-induced pulmonary injury via down-regulating the expression of p38 MAPK in rats. *BMC Complementary and Alternative Medicine* 14: 498.
46. Kim HJ, Kang WY, Seong SJ, et al. (2016) Follistatin-like 1 promotes osteoclast formation via RANKL-mediated NF-κB activation and M-CSF-induced precursor proliferation. *Cell Signal* 28(9): 1137–1144.
47. Guo J, Liang W, Li J, et al. (2016) Knockdown of FSTL1 inhibits oxLDL-induced inflammation responses through the TLR4/MyD88/NF-κB and MAPK pathway. *Biochemical and Biophysical Research Communications* 478(4): 1528–1533.
48. Zhu J, Shen W, Gao L, et al. (2013) PI3K/Akt-independent negative regulation of JNK signaling by MKP-7 after cerebral ischemia in rat hippocampus. *BMC Neuroscience* 14: 1.
49. Park S, Zhao D, Hatanpaa KJ, et al. (2009) RIP1 activates PI3K-Akt via a dual mechanism involving NF-kappaB-mediated inhibition of the mTOR-S6K-IRS1 negative feedback loop and down-regulation of PTEN. *Cancer Research* 69: 4107–4111.
50. Yadav UC, Naura AS, Aguilera-Aguirre L, et al. (2013) Aldose reductase inhibition prevents allergic airway remodeling through PI3K/AKT/GSK3 beta pathway in mice. *PLoS ONE* 8: e57442.
51. Zhang JW, Zhang GX, Chen HL, et al. (2015) Therapeutic effect of Qingyi decoction in severe acute pancreatitis-induced intestinal barrier injury. *World Journal of Gastroenterology* 21(12): 3537–3546.